ORIGINAL ARTICLE

PDCD4 limits prooncogenic neuregulin-ErbB signaling

Juan Carlos Montero[1] · Atanasio Pandiella[1]

Abstract

The neuregulins and their ErbB/HER receptors play essential roles in mammalian development and tissue homeostasis. In addition, deregulation of their function has been linked to the pathogenesis of diseases such as cancer or schizophrenia. These circumstances have stimulated research into the biology of this ligand-receptor system. Here we show the identification of programmed cell death protein-4 (PDCD4) as a novel neuregulin-ErbB signaling mediator. Phosphoproteomic analyses identified PDCD4 as protein whose phosphorylation increased in cells treated with neuregulin. Mutagenesis experiments defined serine 67 of PDCD4 as a site whose phosphorylation increased upon activation of neuregulin receptors. Phosphorylation of that site promoted degradation of PDCD4 by the proteasome, which depended on exit of PDCD4 from the nucleus to the cytosol. Mechanistic studies defined mTORC1 and ERK1/2 as routes implicated in neuregulin-induced serine 67 phosphorylation and PDCD4 degradation. Functionally, PDCD4 regulated several important biological functions of neuregulin, such as proliferation, migration, or invasion.

Keywords Neuregulin · ErbB receptors · Breast cancer · PDCD4

Introduction

The ligands of the epidermal growth factor (EGF) family of polypeptide growth factors and their receptors, the ErbB/HER family of transmembrane tyrosine kinases, play essential roles in animal physiology, and their deregulation has been linked to diseases such as cancer or schizophrenia [1–3]. Therefore, a better knowledge of the signaling through this ligand-receptor system may help in the development of strategies to better approach these diseases.

The Neuregulins (NRGs) comprise the largest subfamily of EGF-like polypeptide growth factors [3]. Functional physiological studies demonstrated that these factors play essential roles in heart and peripheral nervous system development [4–6]. Four NRG genes have been identified in humans, that code for more than 30 different NRG isoforms [3]. As occurs with other EGF family members, most of the NRGs are biosynthesized as membrane-bound precursors, termed proNRGs that may undergo proteolytic cleavage to generate soluble forms [7, 8].

The NRGs act by binding to the ErbB/HER receptor tyrosine kinases. In mammals, four different ErbB/HER receptors have been described: the EGFR/ErbB1/HER1, ErbB2/HER2/neu, ErbB3/HER3 and ErbB4/HER4 [9, 10]. Structurally these receptors are transmembrane proteins which contain a glycosylated extracellular region with four different subdomains, a transmembrane segment in the middle of the molecule, and an intracellular cytosolic region endowed with tyrosine kinase activity. Genetic studies carried out in mice have demonstrated a critical role of these receptors in animal development and homeostasis [11]. Thus, deletion of the EGFR has been shown to provoke skin and central nervous system anomalies [12, 13]. In the case of ErbB2, ErbB3, and ErbB4, their deletion is accompanied by heart disgenesia as well as central and peripheral nervous system neuropathies [14–17].

Several precedents indicate that alterations in the NRG-ErbB system may play a pathophysiological role in diverse types of cancer. A causative action of NRGs in tumor development has been supported by preclinical studies in mice in

---

✉ Juan Carlos Montero
jcmon@usal.es

1 Institute of Biomedical Research of Salamanca (IBSAL), Instituto de Biología Molecular y Celular del Cáncer (CSIC) and CIBERONC, Campus Miguel de Unamuno, 37007 Salamanca, Spain

which overexpression of *NRG1* gene products caused development of mammary adenocarcinomas [18]. In humans, expression of NRGs has been reported in different tumors [3]. In addition, NRG rearrangements have recently been shown in cholangiocarcinomas, lung or pancreatic tumors [19–23]. Importantly, targeting of the NRG-ErbB axis has shown antitumorogenic activity in patients in which such axis was found to be active [24, 25]. Furthermore, expression of NRGs may be used to biomark patients sensitive to therapies that target the NRG-ErbB axis [26, 27].

In the case of the ErbB/HER receptors, gain of function alterations, either by overexpression [1, 28] of molecular alterations [29, 30], have been linked to the genesis/progression of different neoplastic diseases. In humans, increased levels of HER2 occur in a subset of breast and gastric cancers [1, 9]. Pioneering studies in the former also demonstrated a relationship between HER2 levels and patient prognosis [28]. For these reasons, antibodies or small molecule inhibitors of the kinase activity of HER2 have been developed and some of them have reached the oncology clinic. In the case of the EGFR, molecular alterations of this receptor have been reported in a subset of glioblastomas as well as in lung cancer, leading to approval of small molecule kinase inhibitors in the latter pathology. In addition, expression of the EGFR in head and neck, pancreatic and colon cancer also led to the approval of agents that target this receptor for the therapy of those diseases [1, 9].

Because of the relevance of NRG-ErbB signaling axis in cancer, efforts to understand how the NRG-ErbB interaction facilitates tumor generation/progression have and are being made. In this area of research, and using different functional, proteomic and genomic strategies, we have identified several pathways that participate in the prooncogenic actions of the NRG-ErbB axis in human cancer cells. These include the ERK5 mitogen-activated protein kinase route [31]; the GTPase activating protein P-REX1 [32, 33], and the metalloprotease MMP13/Collagenase-3 [34, 35]. Here, by using a proteomic approach, we describe for the first time that programed cell death-4 (PDCD4) is a novel relevant component of the prooncogenic signals activated by the interaction of NRGs with their receptors. We show that activation of NRG receptors rapidly phosphorylates and downregulates PDCD4, actions required for cell cycle progression and cellular motility upon activation of those receptors.

Materials and methods

Reagents and antibodies

Dulbecco's modified Eagle medium (DMEM), fetal bovine serum (FBS), penicillin and streptomycin were purchased from Life Technologies (Carlsbad, CA, USA). Protein-A

Sepharose, phorbol 12-myristate 13-acetate (PMA), 4′, 6-diamidino-2-phenylindole (DAPI), MG132 and 3-(4, 5-dimethylthiazol-2-yl)-2, 5-diphenyltetrazolium bromide (MTT) were from Sigma-Aldrich (St. Louis, MO, USA). Immobilon®-P transfer membrane was from Merck Millipore Corp. (Darmstadt, Germany). Human recombinant Neuregulin-1 β2 was from Prospec Protein Specialists (Rehovot, Israel). Phosphatase alkaline was from Roche Molecular Systems (Madrid, Spain). The phosphoinositide 3-kinase (PI3K) inhibitor PX866 was from Cayman Chemical (Hamburg, Germany). BEZ235, lapatinib, neratinib and rapamycin were from LC Laboratories (Woburn, MA, USA). The MEK inhibitor AZD6244, the AKT inhibitor MK-2206, the p70 ribosomal S6 kinase inhibitor PF-4708671 and the p90RSK inhibitor BI-D1870 were from Selleckchem (Houston, TX, USA). Leptomycin B was from Tocris Bioscience (Bristol, United Kingdom). Other generic chemicals were from Sigma-Aldrich (St. Louis, MO, USA), USB Corporation (Cleveland, OH, USA) Roche Molecular Systems Roche Biochemicals (Hoffmann, Germany), or Merck (Darmstadt, Germany).

Antibodies against MMP13, ERK1/2, PY99 and GAPDH were from Santa Cruz Biotechnology (Santa Cruz, CA, USA). Antibodies against PDCD4, phospho-AKT (Thr308), AKT, phospho-p70S6K (Thr421/Ser424), phospho-ERK1/2 (Thr202/Tyr204), S6 and phospho-S6 (Ser240/244) were from Cell Signaling Technologies (Beverly, MA, USA). The mouse monoclonal anti-phospho-AKT (Ser473) was from BD Pharmingen (Palo Alto, CA, USA). The anti-HER2 antibody used for immunoprecipitation was trastuzumab (Roche). The Ab-3 anti-HER2 antibody used for Western was from Calbiochem. The anti-HA (12CA5) antibody was from Roche Molecular Systems. The rabbit polyclonal anti-calnexin was from Stressgen Bioreagents (Victoria, BC, Canada). The anti pS^{313}-P-REX1 antibody has been described previously [33]. The horseradish peroxidase (HRP)-conjugated anti-mouse, anti-rabbit and anti-rabbit light chain were obtained from GE Healthcare Life Sciences (Piscataway, NJ, USA), Bio-Rad Laboratories (Hercules, CA, USA) and Jackson Immunoresearch Laboratories (West Grove, PA, USA), respectively.

Cell culture, transfections, lentivirus production and infection

MCF7, BT474, SKBR3 and T47D cells were grown in Dulbecco's modified Eagle's medium (DMEM) supplemented with 10% fetal bovine serum (FBS), containing high glucose (4500 mg/l) and antibiotics (penicillin 100 U/ml, streptomycin 100 μg/ml). Cell lines were cultured at 37 °C in a humidified atmosphere in the presence of 5% CO_2, and 95% air. Where indicated, cells at 80% confluence were serum-starved for 16–18 h and pretreated with 0.1% DMSO

(vehicle control) or the different drugs at the concentrated indicated. Subsequently, cells were stimulated or not with 10 nM NRG for the indicated times and collected for protein extraction.

Transfections of MCF7 cells with the plasmids coding for HA-PDCD4-WT and the different PDCD4 mutants were performed with JetPEI DNA transfection reagent (Polyplus-transfection SA, Illkirch, France) following the manufacturer's instructions.

For lentivirus production, 4 μg of the following plasmids: pMDLg/RRE, pRSV-Rev and pMD2.G (Addgene, Cambridge, MA, USA), along with 8 μg of the pLKO.1 lentiviral plasmid containing a scramble shRNA (sh-Control) or the shRNA for PDCD4 (GE Dharmacon, Lafayette, CO, USA) were co-transfected into HEK293T cells using JetPEI® reagent (Polyplus-transfection, Illkirch, France) following the manufacturer's instructions. Twenty-four hours later, HEK293T medium was replaced with fresh medium and 48 h after the co-transfection, the medium containing lentiviral particles was collected, filtered and used to infect MCF7 cells after the addition of 6 μg/ml polybrene (Sigma-Aldrich, St. Louis, MO, USA). MCF7 cells were cultured for 48 h to allow for efficient protein knockdown and were subsequently selected with 3 μg/ml puromycin (Sigma-Aldrich, St. Louis, MO, USA) for another 48 h. A minimum of 5 different shRNA sequences targeting PDCD4 were tested and the two one that produced higher knockdown were used (#957 and #958).

Reverse transcription–PCR assays

Total RNA from MCF7 cells was isolated using TRIzol® reagent (Invitrogen, Carlsbad, CA, USA) according to the manufacturer's instructions. First-strand cDNA was synthesized using M-MLV reverse transcriptase and oligo-dT (Invitrogen) following the instructions from the manufacturer. The oligonucleotides used to amplify PDCD4 were:

FW1 EcoR1: 5′-CGGAATTCATGGATGTAGAAAATG AGCAGATA-3′

RV687: 5′-TGTCCCACAAAGGTCAGAAA-3′

FW623: 5′-CATTGGAGGGGAAGGCTAGT-3′

RV1410XhoI: 5′-CCGCTCGAGTCAGTAGCTCTCTGG TTTAAGACG-3′

Human PDCD4 tagged with an HA epitope at the N-terminus was subcloned into the expression vector pcDNA3 (pcDNA3-HA-PDCD4). Deletions in C-terminus of PDCD4 were generated by site directed mutagenesis using the QuikChange kit (Stratagene, La Jolla, CA, USA) and following the manufacturer's instructions (ΔCt-G318 and ΔCt-C227 deletions). N-terminal deletions were prepared by PCR (ΔNt-D132 and ΔNt-I55 deletions). Other mutants of PDCD4 were generated by oligonucleotide directed mutagenesis. The following oligonucleotides were used:

HA-PDCD4 ΔCt-G318 (FW: 5′-GATAGTGTGTGGGGC TCTTGAGGTGGGCAGCAATCTG-3′; RV: 5′-CAGATT GCTGCCCACCTCAAGAGCCCCACACACTATC-3′).

HA-PDCD4 ΔCt-C227 (FW: 5′-CTTCTTTCTGACCTT TGAGGGACAGTAATGAGCAC-3′; RV: 5′-GTGCTCATT ACTGTCCCTCAAAGGTCAGAAAGAAG-3′).

HA-PDCD4 ΔNt-D132 (FW EcoRI: 5′-CGGAATTCG ATGTGGAGGAGGTGGATGT-3′; RV1410XhoI: 5′-CCG CTCGAGTCAGTAGCTCTCTGGTTTAAGACG-3′.

HA-PDCD4 ΔNt-I55 (FW EcoRI: 5′-CGGAATTCATTA ATGCCAAGGCAAAAAGGC-3′; RV1410XhoI: 5′-CCG CTCGAGTCAGTAGCTCTCTGGTTTAAGACG-3′.

HA-PDCD4 S94A (FW: 5′-GATTAACTGTGCCAACCG CTCCAAAGGGAAGGTTGC-3′; RV: 5′-GCAACCTTC CCTTTGGAGCGGTTGGCACAGTTAATC-3′).

HA-PDCD4 S87A (FW: 5′-GAGTGACGCCCTTAG AGCTGGATTAACTGTGCC-3′; RV: 5′-GGCACAGTT AATCCAGCTCTAAGGGCGTCACTC-3′).

HA-PDCD4 S104A S106A (FW: 5′-GCTGGATAGGCG AGCCAGAGCTGGGAAAGGAAGGG-3′; RV: 5′-CCC TTCCTTTCCCAGCTCTGGCTCGCCTATCCAGC-3′).

HA-PDCD4 S67A S68A (FW: 5′-CGACTAAGGAAA AACGCAGCCCGGGACTCTGGC-3′; RV: 5′-GCCAGA GTCCCGGGCTGCGTTTTTCCTTAGTCG-3′).

HA-PDCD4 S71A (FW: 5′-GAAAAACTCATCCCG GGACGCTGGCAGAGGCGATTC-3′; RV: 5′-GAATCG CCTCTGCCAGCGTCCCGGGATGAGTTTTTC-3′).

HA-PDCD4 S76A S78A (FW: 5′-CTGGCAGAGGCG ATGCGGTCGCCGACAGTGGGAGTG-3′; RV: 5′-CAC TCCCACTGTCGGCGACCGCATCGCCTCTGCCAG-3′).

HA-PDCD4 S80A S82A (FW: 5′-GATTCGGTCAGC GACGCTGGGGCTGACGCCCTTAGAAG-3′; RV: 5′-CTT CTAAGGGCGTCAGCCCCAGCGTCGCTGACCGAA TC-3′).

HA-PDCD4 S67A (FW: 5′-CGACTAAGGAAAAAC GCATCCCGGGACTCTGGC-3′; RV: 5′-GCCAGAGTC CCGGGATGCGTTTTTCCTTAGTCG-3′).

HA-PDCD4 S68A (FW: 5′-CGACTAAGGAAAAAC TCAGCCCGGGACTCTGGC-3′; RV: 5′-GCCAGAGTC CCGGGCTGAGTTTTTCCTTAGTCG-3′).

Generation of antibodies, immunoprecipitation, Western blotting and immunofluorescence

The anti-PDCD4 antibody was raised in rabbits against the sequence NH2-CVSEGDGGRLKPESY-COOH that corresponds to the amino acids 456–469 located at the C-terminus of PDCD4. The antibody was affinity purified using peptide-Sepharose columns. The generation of anti-pS^{313}-P-REX1 has been described [33]. The procedures for the preparation of cell extracts for protein analyses, immunoprecipitation and Western blotting have been described [36, 37]. GAPDH or calnexin were used as a loading

controls. Densitometric measurements of the bands were performed using the public domain ImageJ program (NIH, Bethesda, MD, USA) or Image LabTM Software Version 6.0.1 Bio-Rad Laboratories (Hercules, CA, USA), which was provided with a ChemiDoc apparatus. The immunofluorescence protocol has been described [31]. Dilutions of the anti-PDCD4 or anti-HA antibodies were 1:500 and 1:200, respectively. Quantitation of nuclear or cytoplasmic PDCD4 was carried out using ImageJ with the gaussian mask tool to define nuclear areas. A minimum of five different randomly selected microscopic fields were analyzed for each condition.

Dephosphorylation assays

Extracts (40 μg) of MCF7 cells stimulated with or without NRG were treated with or without 3 units of phosphatase alkaline (Roche) in dephosphorylation buffer (50 mM Tris–HCl, 0.1 mM EDTA, pH 8.5) (Roche) at 37 °C during 5 h. On the other hand, extracts of MCF7 cells treated with or without NRG were immunoprecipitated with anti-PDCD4. The immunocomplexes were washed thrice with lysis buffer and three times with dephosphorylation buffer (50 mM Tris–HCl, 0.1 mM EDTA, pH 8.5) and then treated with 3 units of phosphatase alkaline in dephosphorylation buffer for 3 h at 37 °C. The reactions were terminated by adding sample buffer, and the samples were analyzed by Western blotting using anti-pS^{313}-P-REX1 antibodies.

Cell proliferation, wound healing and cell invasion assay

Cell proliferation was assessed by MTT metabolization as previously described [34]. For cell migration analysis, the wound healing assay was performed as described previously [33]. After NRG stimulation, images were captured until the wound in NRG-stimulated cells fully sealed or for a maximum of 48 h with a Nikon Eclipse TE2000-E inverted microscope (Nikon Corporation, Chiyoda-ku, Tokyo, Japan) equipped with the MetaMorph® Microscopy Automation and Image Analysis Software (Molecular Devices LLC, Sunnyvale, CA, USA). The area between the wound edges was measured using the ImageJ program (NIH, Bethesda, MD, USA) and relativized to the initial area. The cell invasion assay was performed as previously described [33]. The number of invading cells was counted under a Nikon Eclipse Ti-S inverted microscope (Nikon Corporation, Chiyoda-ku, Tokyo, Japan) using the ProgRes® CapturePro 2.7 program (Jenoptik AG, Jena, Germany). Results are presented as the mean ± SD of triplicates of a representative experiment that was repeated three times.

Protein and phosphorylated peptides identification

To identify p60, MCF7 cells stimulated with or without NRG were washed with phosphate-buffered saline and fractionated into microsomal and cytosolic fractions [8]. Cytosolic fractions were loaded in a column that contained a matrix for the purification of phosphopeptides (PhosphoCruz Protein Purification System, Santa Cruz Biotechnology). The eluates were concentrated and subjected to 2D PAGE. The gels were transferred to Immobilon P membranes that were blocked in Tris-buffered saline with Tween (TBST) (100 mM Tris [pH 7.5], 150 mM NaCl, 0.05% Tween 20) containing 1% of bovine serum albumin for 1 h and then incubated with the anti- pS^{313}-P-REX1- antibody for 2–16 h. After washing with TBST, membranes were incubated with HRP-conjugated anti-rabbit secondary antibodies (1:10,000 dilution) for 30 min and bands were visualized by using ECL Plus Western Blotting Detection System (GE Healthcare, Buckinghamshire, United Kingdom). The region of the PVDF membrane where the signal of the p60 band migrated was excised and digested with trypsin. The protein peptide mass fingerprint was obtained on an Orbitrap Ultraflex MALDI-TOF mass spectrometer (Bruker Daltonics, Brenen, Germany) and Mascot search engine (Matrix Science, London, UK) against Swiss-Prot database was used to identify proteins. One result was considered to be significant ($P < 0.05$) when the protein score value exceeded 56.

Statistical analyses

Data were analyzed statistically using the software package SPSS 15.0 (SPSS Inc. Chicago, IL, USA). Comparison of continuous variables between two groups for in vitro assays were performed using a two-sided Student's t test. Differences were considered statistically significant when P value was less than 0.05. All experiments were repeated at least twice. Representative results of all the findings are shown.

Results

NRG provokes phosphorylation of a 60-kDa protein

Due to the relevance of the ErbB/HER receptors in cancer and animal biology, significant efforts have and are being made to understand the signaling pathways activated by these transmembrane tyrosine kinases. Using a phosphoproteomic approach, we formerly identified P-REX1 as an intermediate of the NRG-ErbB signaling axis [33]. It was reported that stimulation of ErbB receptors with NRGs engages a phosphorylation/dephosphorylation cycle that causes dephosphorylation of serines 313 and 319 of P-REX1 and concomitant phosphorylation of serines 605 and 1169.

Those phosphorylation changes result in increased guanine nucleotide exchange activity of P-REX1 [33, 38]. While analyzing this phosphorylation/dephosphorylation cycle of P-REX1, we observed that an antibody that we generated against P-REX1 phosphorylated at serine 313 also recognized a band of 60 kDa (p60) in MCF7 breast cancer cells treated with NRG (Fig. 1a). As that antibody was raised against phosphorylated P-REX1 ([33], see also Fig. 2i), the possibility that the 60 kDa protein resulted from proteolytic cleavage of whole length P-REX1 was contemplated. To explore that, lysates from control or NRG-treated MCF7

cells were immunoprecipitated with the anti-pS^{313}-P-REX1 antibody and blotted with the same antibody. As shown in Fig. 1a, treatment with NRG decreased the electrophoretic mobility of P-REX1, indicative of increase in its overall phosphorylation. However, the phosphorylation at Ser^{313} slightly decreased upon treatment with NRG, in agreement with previously published data [33]. In the case of p60, while NRG increased its recognition by the anti-pS^{313}-P-REX1 antibody in cell extracts, it was not precipitated by the anti-pS^{313}-P-REX1 antibody, while P-REX1 was. These data excluded, together with additional Western experiments
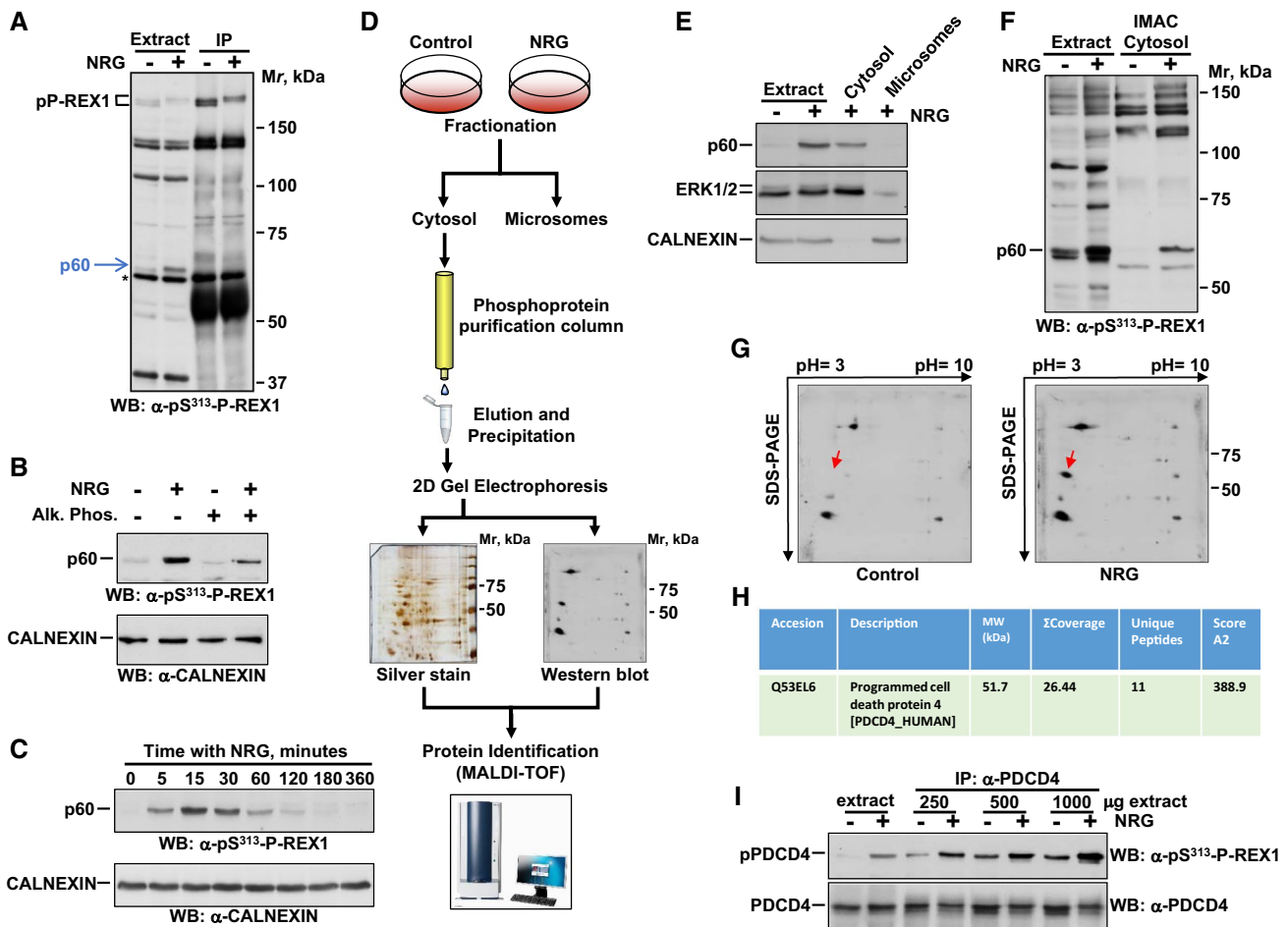

Fig. 1 Identification of a novel NRG-ErbB intermediate. **a** MCF7 cells stimulated with or without NRG (10 nM) for 15 min were lysed and cell extracts or anti-P-REX1 immunoprecipitates analyzed by Western blot with an anti-pS^{313}-P-REX1 antibody. The position of the M_r markers is shown at the right. **b** p60 is phosphorylated. Extracts from MCF7 cells stimulated with or without NRG were treated with alkaline phosphatase and the samples were analyzed by Western with the anti-pS^{313}-P-REX1 antibody. Calnexin was used as a loading control. **c** Kinetics of phospho-p60 in response to NRG. Lysates from MCF7 cells treated for different times with NRG were analyzed by Western with the anti-pS^{313}-P-REX1 antibody. **d** Schematic representation of the steps used to identify p60. **e** p60 is a cytosolic protein. MCF7 cells treated or not with NRG were homogenized and the

cytosolic and microsomal fractions analyzed by Western blot with the anti-pS^{313}-P-REX1 antibody. ERK1/2 and calnexin were used as controls of cytosolic or microsomal fractions, respectively. **f** Analysis of p60 in eluates from phosphopeptide purification IMAC columns. **g** After preparation of cytosolic fractions from control and NRG-treated MCF7 cells, eluted phosphoproteins were precipitated and resolved in 2D gels that were then transferred to PVDF membranes. p60 was detected in these blots with the anti-pS^{313}-P-REX1 antibody. Red arrows indicate p60. **h** The table shows the main protein identified in the proteomic analysis of the region corresponding to p60. **i** p60 is PDCD4. Cell extracts from MCF7 cells treated with or without NRG were inmunoprecipitated with anti-PDCD4 antibodies
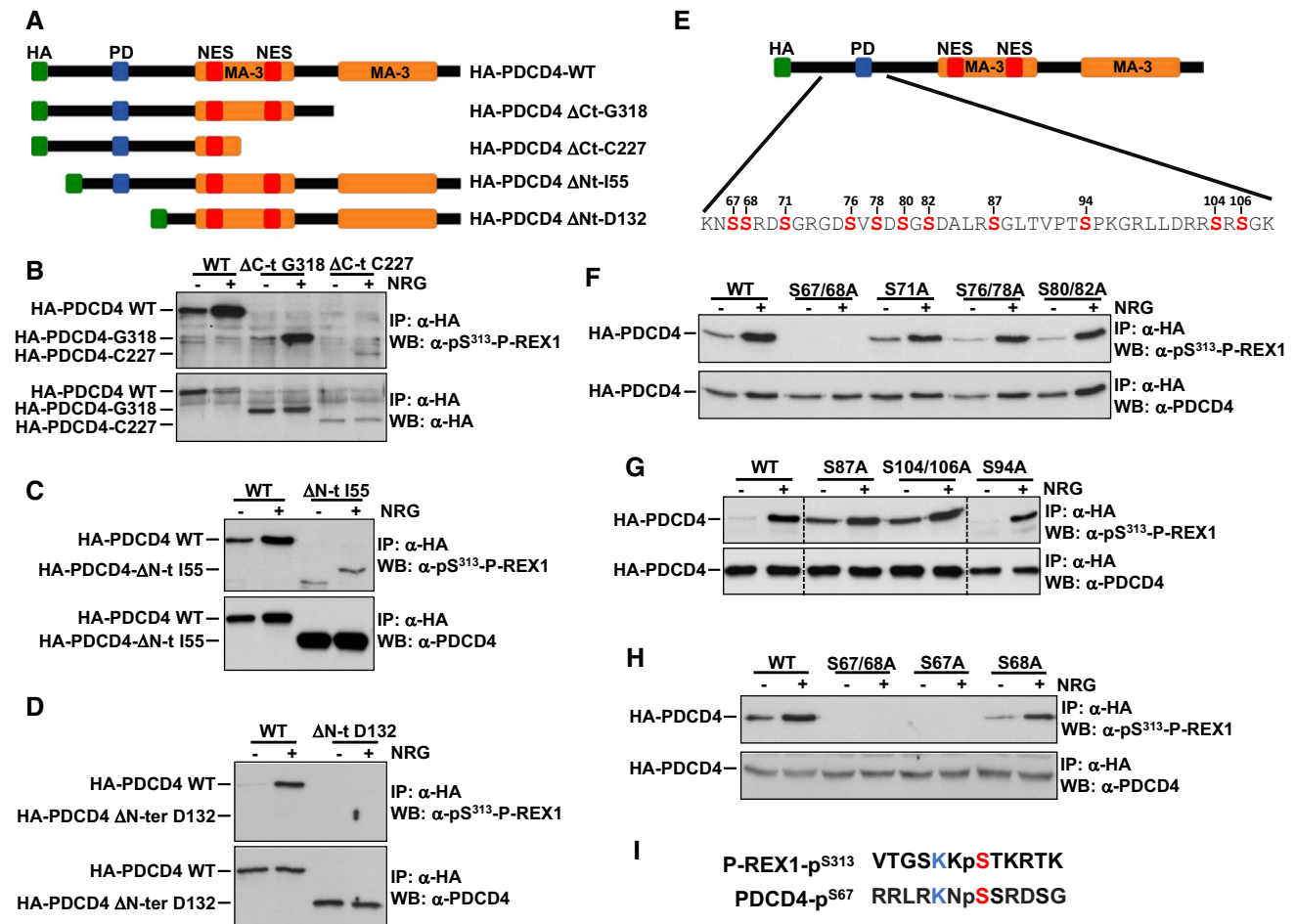
Fig. 2 The anti-pS313-P-REX1 antibody cross-reacts with pSer67 in PDCD4. **a** Schematic representation of different domains of HA-tagged wild type PDCD4 and different deletion mutants. HA: hemagglutinin, PD: phosphodegron (aa 70–76), the MA-3 domains are in orange (aa 163–284 and aa 326–449), red boxes are the potential nuclear export signals (NES), aa 241–251 and aa 182–192. **b**–**d** MCF7 cells transfected with HA-tagged wild type PDCD4 or HA-PDCD4 deletion mutants in: ΔC-t G318, ΔC-t C227 (**b**), ΔN-t I55 (**c**) or ΔN-t D132 (**d**) were treated without or with NRG (10 nM). Cell extracts were immunoprecipitated with the anti-HA antibody and the blots were probed with the indicated antibodies. **e** Serines present in the region spanning amino acids 55 and 132. **f**–**h** MCF7 cells transfected with wild type HA-PDCD4 or different mutants in which serine residues were replaced by alanine were treated with or without NRG. Cell extracts were immunoprecipitated with anti-HA and the blots were probed with anti-pS313-P-REX1. These blots were reprobed with the anti-PDCD4 antibody. **i** Sequence of P-REX1 used to generate the anti-pS313-P-REX1 antibody, aligned to the region surrounding S67

carried out with other antibodies directed to different regions of P-REX1 (data not shown) that p60 resulted from proteolytic fragmentation of P-REX1.

Another set of experiments were designed to define whether p60 was pAKT. Such possibility was contemplated since P-REX1 was initially isolated because of its cross-reactivity with an anti-pSer473-AKT antibody [33], and also by the fact that AKT has a molecular weight close to p60. As shown in supplementary Fig. 1a, immunoprecipitated AKT was not recognized by the anti-pS313-P-REX1 antibody. However, pAKT was recognized by an anti-pSer473-AKT antibody (supplementary Fig. 1b). Recognition of p60 by the anti-pS313-P-REX1 antibody was dependent on its phosphorylation, since treatment of cell extracts with alkaline

phosphatase substantially decreased the reactivity of the 60 kDa band with the anti-pS313-P-REX1 antibody (Fig. 1b). Time-course experiments in MCF7 cells treated with NRG showed that phosphorylation of p60 rapidly reached a peak at 15 min of stimulation with NRG, and then decreased over time (Fig. 1c).

Identification of p60 as PDCD4

In addition to showing that p60 was different from P-REX1 or AKT, the above experiments also demonstrated that p60 could not be precipitated by the anti-pS313-P-REX1 antibody. That characteristic hampered one step immunopurification of p60 with the aim of its identification. Because of

that, we followed a strategy, schematized in Fig. 1d, similar to the one formerly used to identify P-REX1 as a NRG-ErbB signaling mediator [33]. Such strategy started with a cell fractionation step to define whether p60 was a cell membrane-bound or cytosolic protein. These experiments showed that p60 was cytosolic, as it fractionated with the cytosolic proteins ERK1 and ERK2, but not with the integral endoplasmic reticulum membrane protein calnexin (Fig. 1e). Next, we used the cytosolic fraction of control or NRG-stimulated MCF7 cells to enrich for phosphorylated proteins using immobilized metal affinity (IMAC) based columns. Proteins in the eluates from these columns were precipitated and run on SDS-PAGE gels. Western blotting of those eluates confirmed the presence of p60 along this enrichment process (Fig. 1f). The precipitated proteins from the IMAC column eluates were also run on 2D gels, which were silver stained, and the region corresponding to p60 subjected to mass spectrometry analysis (supplementary Fig. 1c). These analyses resulted in the identification of several proteins that could correspond to p60. Because of their molecular weight and subcellular distribution, we initially focused on two of them, the pyruvate kinase isozyme M1 and the serine/threonine protein phosphatase 2A (supplementary Fig. 1c). However, immunoprecipitation of cell lysates with antibodies towards these proteins followed by Western with the anti-pS^{313}-P-REX1 antibody failed to define them as p60 (data not shown).

We then took a slightly different approach based on the direct analysis of p60 in Westerns from 2D gels, instead of cutting the region in the polyacrylamide gel to perform proteomic analysis. Thus, after 2D electrophoresis, gels were transferred to PVDF membranes that were probed with anti-pS^{313}-P-REX1. After Western identification of p60, the region of the PVDF membrane was excised and processed to be analyzed by mass spectrometry. We decided to do that protocol to more precisely select the region of the 2D gels where p60 migrated (Fig. 1g). These experiments led to the identification of the programmed cell death protein-4 (PDCD4) as the potential p60 (Fig. 1h). That protein was in fact one of the proteins detected by the initial proteomic studies (see the table shown in supplementary Fig. 1c) of the silver-stained 2D gels but was excluded from our initial analyses because its expected molecular weight of 51.7 kDa was below the expected 60 kDa weight of p60.

To analyze if PDCD4 was the protein recognized by the anti-pS^{313}-P-REX1 antibody, we raised an antibody to PDCD4 which was used to immunoprecipitate PDCD4. Using that reagent, PDCD4 was immunoprecipitated from cellular extracts of MCF7 cells and the precipitates analyzed by Western blot using the anti-pS^{313}-P-REX1 or anti-PDCD4 antibodies. PDCD4 was detected by the anti-pS^{313}-P-REX1 antibody, indicating that the phosphorylated 60 kDa band corresponded to PDCD4 (Fig. 1i). Furthermore, PDCD4

immunoprecipitated from NRG-treated MCF7 cells and treated with alkaline phosphatase was weakly detected by the anti-pS^{313}-P-REX1 antibody, indicating that this antibody recognized PDCD4 when phosphorylated (supplementary Fig. 1d).

The anti-pS^{313}-P-REX1-antibody recognizes pSer^{67} in PDCD4

To find out the serine(s) recognized by the anti-pS^{313}-P-REX1 antibody, different regions of PDCD4 were truncated. Two C-terminal region deletions as well as another two N-terminal deletions of PDCD4 were prepared (Fig. 2a). These mutants were transfected in MCF7 cells and the cells were stimulated with NRG. C-terminal deletions of PDCD4 failed to prevent interaction of the truncated proteins with the anti-pS^{313}-P-REX1 antibody (Fig. 2b). Analogously, deletion of the first N-terminal 55 amino acids did not prevent identification of the truncated protein by that antibody (Fig. 2c). However, the anti-P-REX1-pS^{313} antibody failed to detect pPDCD4 in the mutant in which the first 132 amino acids were eliminated (Fig. 2d), indicating that the phosphorylated serine residue recognized by the antibody must be in a region between amino acids 55 and 132 of PDCD4. Next, site directed mutagenesis of the serines in the 55–132 region was performed (Fig. 2e). The anti-pS^{313}-P-REX1 antibody was able to recognize PDCD4 in all mutants, except for the double mutant S67/68A (Fig. 2f, g). Separate experiments individually mutating serine 67 and serine 68 to alanine showed that the residue recognized by the anti-P-REX1-pS^{313} antibody corresponded to serine 67 (Fig. 2h). Of note, comparison of the primary sequence used for the generation of the phosphorylated-P-REX1 antibody and that surrounding serine 67 of PDCD4 showed very limited identity (Fig. 2i).

Next, we explored whether serine 67 phosphorylation of PDCD4 was a general effect in the signaling by the NRG-ErbB system. To that end, we used the additional breast cancer cell lines T47D, BT474 and SKBR3. The latter two are representative of HER2+ breast cancer, while the former, together with MCF7, are used as models of the hormonal subtype of breast cancer. All four cell lines express NRG receptors and respond to NRG by activation of the PI3K/mTOR/AKT and RAS/RAF/ERK routes (supplementary Fig. 2a). Addition of NRG caused serine 67 phosphorylation of PDCD4 in all of them except in SKBR3 cells. The lack of effect in the latter cell line could be due by its low resting levels of PDCD4 (supplementary Fig. 2a). The low resting levels observed in SKBR3 cells could be increased by agents such as lapatinib and neratinib, which inhibited HER2 activity, indicating that the high resting levels of pHER2 present in these HER2-overexpressing cell line could constitutively induce down regulation of PDCD4 (supplementary Fig. 2b).

S[67] phosphorylation of PDCD4 is required for NRG-induced degradation of PDCD4

Having discovered that NRG regulates phosphorylation of PDCD4, we then initiated a series of experiments aimed at exploring the relevance of that protein and its S[67] phosphorylation in signaling by NRG receptors.

Time course experiments demonstrated that treatment of MCF7 (Fig. 3a), T47D (supplementary Fig. 3a) or BT474 (supplementary Fig. 3b) cells with NRG did not affect the total amount of PDCD4 at early time points (up to 30 min) but substantially decreased its amount at 60 min of treatment and beyond. At early stimulation times, NRG increased S[67] phosphorylation of PDCD4. However, down regulation of

PDCD4 levels at late incubation times with NRG affected S[67] phosphorylation of PDCD4. Parallel immunofluorescence experiments with an anti-PDCD4 antibody showed that under resting conditions PDCD4 was mainly located in the nucleus and cytosol of MCF7, T47D and BT474 cells (Fig. 3b; supplementary Fig. 3c, d). Two clear effects of NRG on the immunofluorescent signal of PDCD4 were observed. First, at early times of treatment, NRG provoked movement of PDCD4 from the cytosol to the nucleus (Fig. 3b; supplementary Fig. 4a–d). Second, and in line with the Western blotting results, these immunofluorescence studies also showed that the amount of PDCD4 progressively decreased with time of treatment with NRG (Fig. 3b; supplementary Fig. 3c, d).
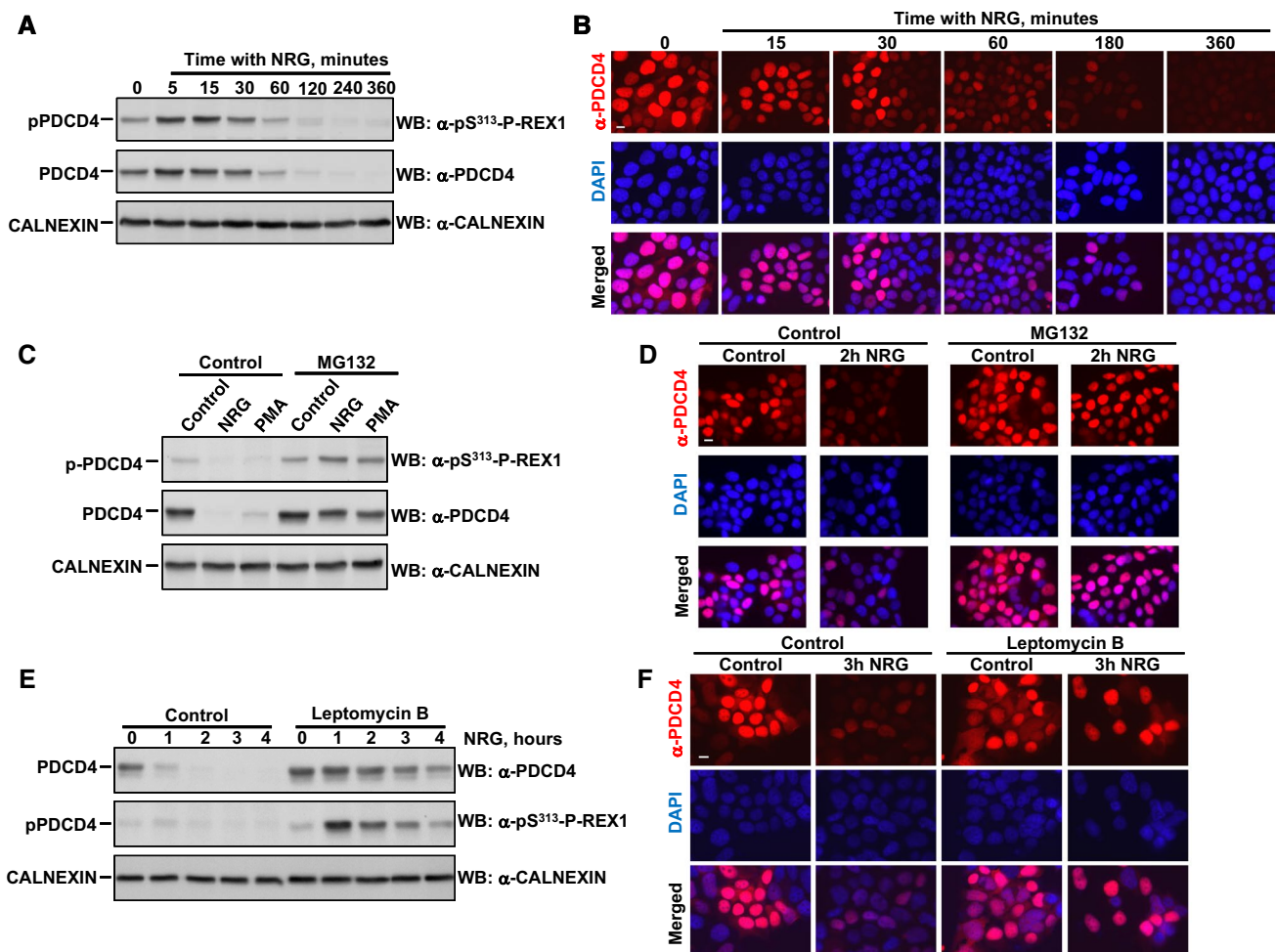

Fig. 3 Role of the proteasome and nucleocytoplasmic circulation in the regulation of PDCD4 levels by NRG receptors. **a** MCF7 cells were treated with NRG for the indicated times. Lysates were analyzed by Western blot with anti-pS[313]-P-REX1 and anti-PDCD4 antibodies. **b** Immunofluorescence analysis of levels of PDCD4 in MCF7 cells treated with NRG. Cells were stained for PDCD4 (red) and DNA (blue). Scale bar = 10 μm. **c**, **d** NRG induces the degradation of PDCD4 via proteasome. MCF7 cells were pre-treated with or without MG132 (10 μM) and then stimulated with NRG or PMA (1 μM) during 6 h (**c**), or with NRG during 2 h (**d**). **e**, **f** Degradation of PDCD4 requires exit to the cytosol. MCF7 cells were pre-treated with leptomycin B (20 μg/ml) and then stimulated with NRG at different times. Analyses of total and pS[67]-PDCD4 were performed by Western blot (**e**), and localization and levels of PDCD4 were analyzed by immunofluorescence (**f**)

Previous reports have indicated that the ubiquitin–proteasome pathway contributes to the regulation of PDCD4 levels in mitogen-deprived cells stimulated with serum or the tumor promoter Phorbol-12-myristate, 13-acetate (PMA) [39–41]. As shown in Fig. 3c, preincubation of MCF7 cells with the proteasome inhibitor MG132 prevented the reduction of PDCD4 levels induced by a 6 h treatment with NRG or PMA. Under these experimental conditions, the levels of pS^{67}-PDCD4 were maintained in cells treated with NRG or PMA. Similar results were obtained in T47D and BT474 cells (supplementary Fig. 4e, f). Immunofluorescence experiments confirmed that MG132 inhibited the degradation of PDCD4 (Fig. 3d).

To explore whether NRG-induced degradation of PDCD4 requires export outside the nucleus, MCF7 cells were preincubated with leptomycin B, which prevents the exit of proteins from the nucleus to the cytosol [42, 43]. Treatment with leptomycin B prevented the degradation of PDCD4 induced by NRG in MCF7 cells (Fig. 3e, f). On the other hand, the phosphorylation of PDCD4 in S^{67} induced by NRG was substantially higher in cells treated with leptomycin B, indicating that the phosphorylation in this residue is maintained in the nucleus because PDCD4 is not degraded, and perhaps not easily accessible to the dephosphorylating phosphatases.

To define whether S^{67} phosphorylation of PDCD4 had a role in its NRG-induced degradation, HA-tagged forms of wild type PDCD4 as well as a mutated form in which S^{67} was replaced by alanine were transfected into MCF7 cells. Immunofluorescence analyses demonstrated that the subcellular distribution of HA-tagged wild type PDCD4 as well as HA-PDCD4-S^{67}A were similar to endogenous PDCD4 (Fig. 4a). Short term treatment with NRG provoked accumulation of HA-tagged wild type PDCD4 and HA-PDCD4-S^{67}A in the nucleus (Fig. 4a), suggesting that phosphorylation of S^{67} was not required for PDCD4 nuclear translocation. Activation of NRG receptors decreased the levels of HA-tagged wild type PDCD4 (Fig. 4b, c). However, the levels of HA-tagged PDCD4-S^{67}A did not decrease over the time of treatment with NRG. Endogenous PDCD4 expression levels decreased with NRG treatment in a similar manner in both cells. These results indicated that phosphorylation of PDCD4 in S^{67} is required for its degradation upon activation of NRG receptors in MCF7 cells.

NRG controls PDCD4 S^{67} phosphorylation and stability through several signaling routes.

The PI3K/mTOR route through the AKT and p70S6K kinases, as well as the ERK1/2 route through p90RSK have formerly been implicated in the regulation of PDCD4 phosphorylation [39–41, 44]. To explore the contribution of both routes to NRG-induced S^{67}PDCD4 phosphorylation,

drugs that target different components of these signaling pathways were used (Fig. 5a). Western blotting experiments confirmed that NRG activated phosphorylation of S6 and AKT, which are used as readouts of activation of the mTORC1 and mTORC2 branches of the PI3K/mTOR pathway, respectively (Fig. 5b). These studies also showed that NRG activated the ERK1/2 route, as indicated by the dual phosphorylation of ERK1/2. Inhibitors targeting upstream components of both routes such as BEZ235, a dual PI3K/mTOR inhibitor, and AZD6244, a highly selective inhibitor of the ERK1/2 upstream activating kinases MEK1/2 were tested. Preincubation with AZD6244 prevented NRG-induced phosphorylation of ERK1/2, without affecting the activatory effect of NRG on S6 or AKT (Fig. 5b). On the other hand, BEZ235 completely inhibited the capability of NRG to provoke increases in pAKT and pS6. With respect to the action of the drugs on the phosphorylation of PDCD4 in S^{67}, each of these drugs used individually slightly reduced the phosphorylation of that residue upon NRG stimulation (Fig. 5b, c). However, combination of AZD6244 with BEZ235 completely abrogated NRG-induced S^{67}PDCD4 phosphorylation. Analogously to that data obtained in MCF7 cells, the combination of AZD6244 with BEZ235 completely inhibited NRG-induced S^{67}PDCD4 phosphorylation in T47D cells (supplementary Fig. 5a).

The above data demonstrated that signals transduced through the PI3K/mTOR and the ERK1/2 routes could control phosphorylation of PDCD4 at S^{67}. Considering this, and former reports which pointed to AKT and p70S6K as kinases capable of phosphorylating S^{67} in PDCD4 [39, 40, 44], the action of inhibitors of these kinases on NRG-induced phosphorylation of PDCD4 at serine 67 was explored. The contribution of p90RSK, which can be activated through the ERK1/2 pathway, was evaluated using BI-D1870 [45], since serine 67 lies in a consensus sequence region that may be targeted by such kinase [46]. That drug had a partial inhibitory effect on NRG-induced phosphorylation of PDCD4 at S^{67} (Fig. 5c). However, when combined with BEZ235, inhibition of NRG-induced phosphorylation of PDCD4 at S^{67} was complete. On the other hand, preincubation with the AKT inhibitor MK-2206 [47], which prevented phosphorylation of AKT activating residues threonine 308 and serine 473 [47], failed to inhibit NRG-induced S^{67}PDCD4 phosphorylation (supplementary Fig. 5b; Fig. 5d). Moreover, treatment with the AKT inhibitor appeared to increase PDCD4 phosphorylation in S^{67}. The failure of MK-2206 to inhibit NRG-induced phosphorylation of PDCD4 at S^{67} was surprising, given the reported role of AKT as a PDCD4 kinase [44], and the results obtained with BEZ235. However, since BEZ235 affected signaling through both mTORC1 and mTORC2 (Fig. 5a, b), the possibility that the mTORC1 branch of the mTOR route was participating in NRG-induced phosphorylation of PDCD4 at S^{67} was

Fig. 4 Phosphorylation of PDCD4 in serine 67 is required for NRG-induced degradation. **a** Phosphorylation of PDCD4 in serine 67 is not required for the cytosol to nucleus transit of PDCD4 induced by NRG. MCF7 cells transfected with wild type HA-PDCD4 or HA-PDCD4-S67A were seeded on coverslips and treated with NRG (10 nM, 15 min). Location of exogenous HA-PDCD4 and endogenous PDCD4 were performed by immunofluorescence. **b** MCF7 cell transfected as above were treated with NRG for times indicated. Levels of HA-PDCD4, HA-PDCD4-S67A and endogenous PDCD4 were analyzed by Western. GAPDH was used as a loading control. **c** Quantitative analysis of the relative protein levels of HA-PDCD4-WT and HA-PDCD4-S67A of the experiment shown in **b**. The numbers indicate hours of treatment with NRG
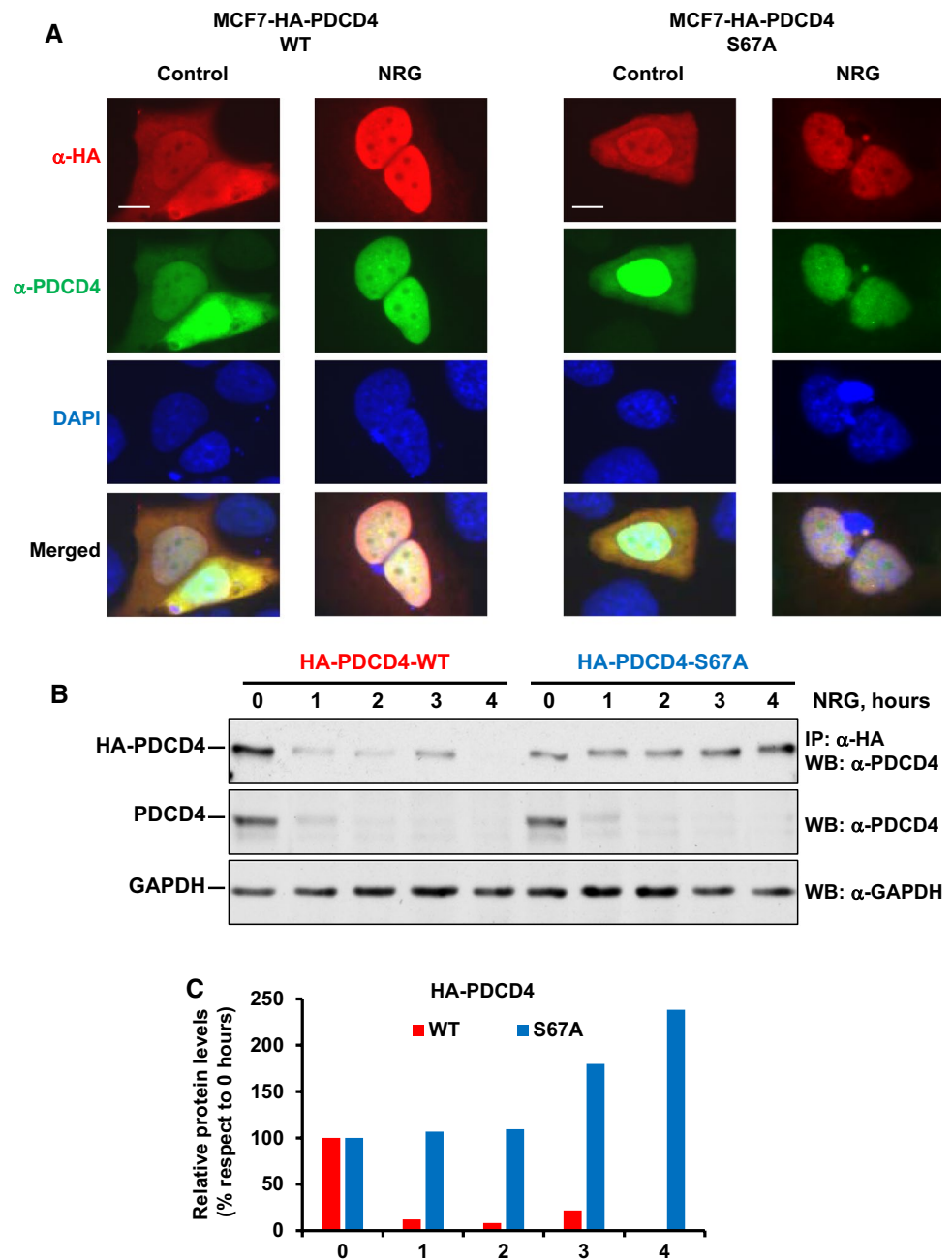
explored. To that end, we used rapamycin, an inhibitor of the mTORC1 complex [48]. Rapamycin alone had little effect on NRG-induced phosphorylation of PDCD4 at S^{67} (Fig. 5d). In contrast, the combination of rapamycin and BI-D1870 fully prevented such phosphorylation. Western blotting analyses demonstrated that rapamycin prevented pS6 but not pAKT phosphorylation, confirming the preferential inhibition of the mTORC1 route by the drug.

To explore whether S6K participated as a downstream intermediate of mTORC1, the inhibitor PF-4708671 was used. By itself, this inhibitor had a discrete inhibitory effect on resting S^{67}PDCD4 phosphorylation, but no appreciable effect on NRG-induced phosphorylation of that residue (supplementary Fig. 5c). However, its combination with the p90RSK inhibitor profoundly inhibited NRG-induced phosphorylation of PDCD4 in S^{67} (supplementary Fig. 5d). Combination of PF-4708671 and AZD6244 prevented NRG-induced phosphorylation of PDCD4 in S^{67} (Fig. 5e). Together, the above studies indicated that the PI3K/mTORC1/S6K and the ERK1/2-p90RSK routes coordinately transduced the signal emanating from the NRG receptors to regulate S^{67} PDCD4 phosphorylation.

Next, the signaling pathways regulating PDCD4 protein levels were explored. BEZ235 and AZD6244 inhibited
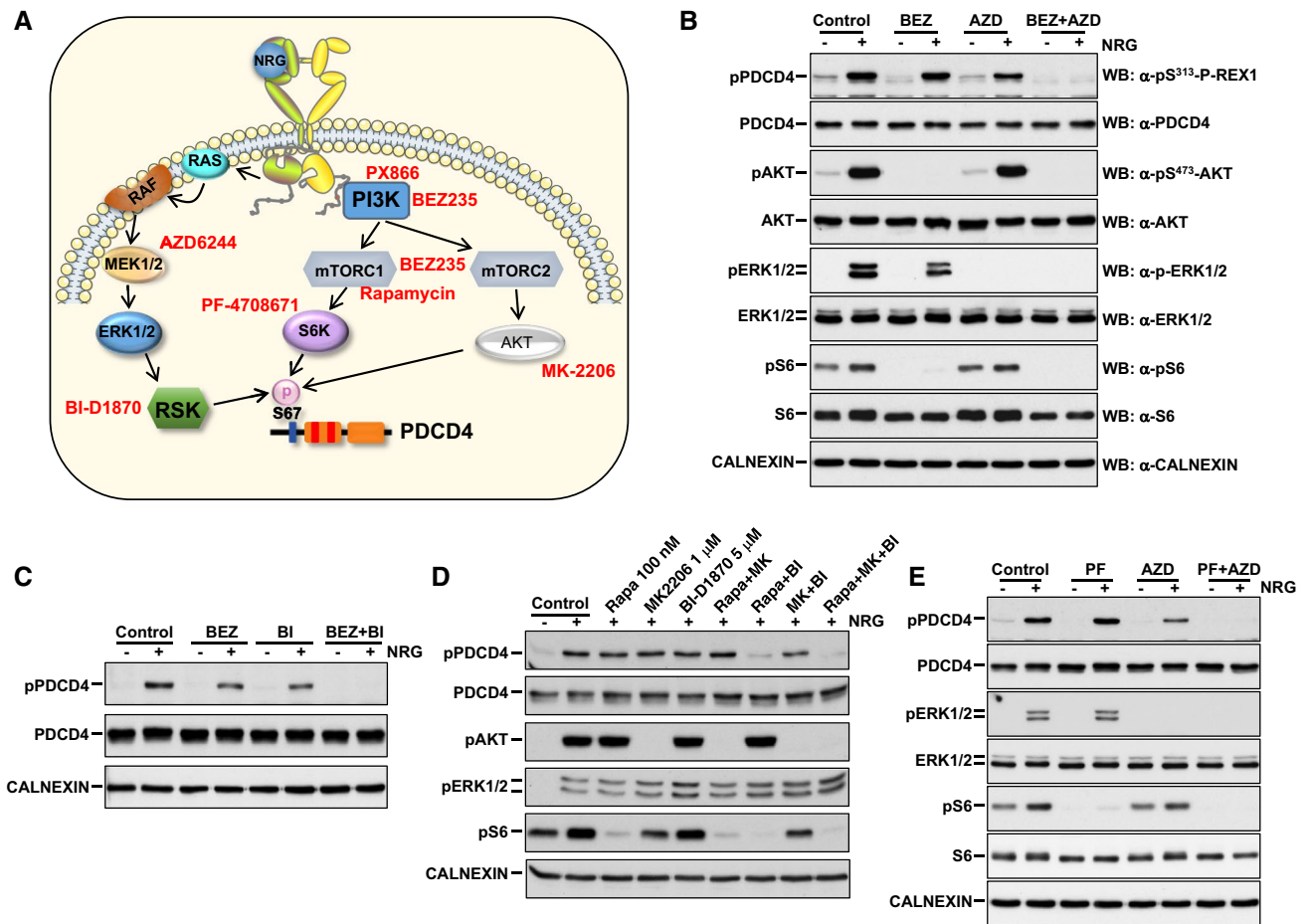
Fig. 5 NRG controls phosphorylation of serine 67 through several signaling routes. **a** Schematic representation of pathways activated by neuregulin-ErbB receptors and analyzed using drugs that block them (shown in red). **b–e** MCF7 cells were preincubated with BEZ235 (1 μM), AZD6224 (5 μM), combination of BEZ235 plus AZD6224, BI-D1870 (5 μM), combination of BEZ235 plus BI-D1870, rapamy- cin (100 nM), MK2206 (1 μM), BI-D1870 (5 μM), rapamycin plus MK2206, rapamycin plus BI-D1870, MK2206 plus BI-D1870, triple combination of rapamycin, MK2206 plus BI-D1870, PF-4708671 (20 μM), AZD6224 (5 μM), and combination of PF-4708671 plus AZD6224. All preincubations with the drugs were for 3 h and treatments with NRG (10 nM) for 15 min

NRG-induced degradation of PDCD4 (Fig. 6a, b; supplementary Fig. 6a), the former having a stronger inhibitory effect. Treatment with these drugs slightly augmented resting PDCD4 levels (supplementary Fig. 6a). The alternative PI3K inhibitor PX866 also prevented NRG-induced degradation of PDCD4 (supplementary Fig. 6b). Time course studies demonstrated the stabilization of PDCD4 levels by BEZ235 (Fig. 6c), which was accompanied by inhibition of pS6 phosphorylation, indicating full inhibition of NRG-induced signaling through the mTORC1 branch. Rapamycin exerted an inhibitory effect similar to BEZ235 on NRG-induced degradation of PDCD4, further supporting that the mTORC1 route controlled such degradation (Fig. 6d). BEZ235 inhibited degradation of PDCD4 triggered by NRG stimulation in several other breast cancer cell lines (supplementary Fig. 6c), confirming that the PI3K/mTOR route controls stability of PDCD4.

PDCD4 is a key element in NRG-induced migration, invasion and proliferation.

PDCD4 has formerly been implicated in migration of cancer cells [49]. Since this biological characteristic can be regulated by NRGs [3], the potential participation of PDCD4 in that response was investigated. To that end, the levels of PDCD4 were first decreased using RNA interference (Fig. 7a). When MCF7-sh-control and MCF7-sh-PDCD4 cells reached confluence, the surface of the monolayers was scratched with a pipette tip to create an area without cells (Fig. 7b). Then, cells were serum-deprived and treated with or without NRG. Photographs of the wounded regions of the dishes were obtained at days 0, 1 and 2 (Fig. 7b; supplementary Fig. 7a). MCF7 cells in which the levels of PDCD4 were decreased migrated more than the parental MCF7 cell line, especially in the
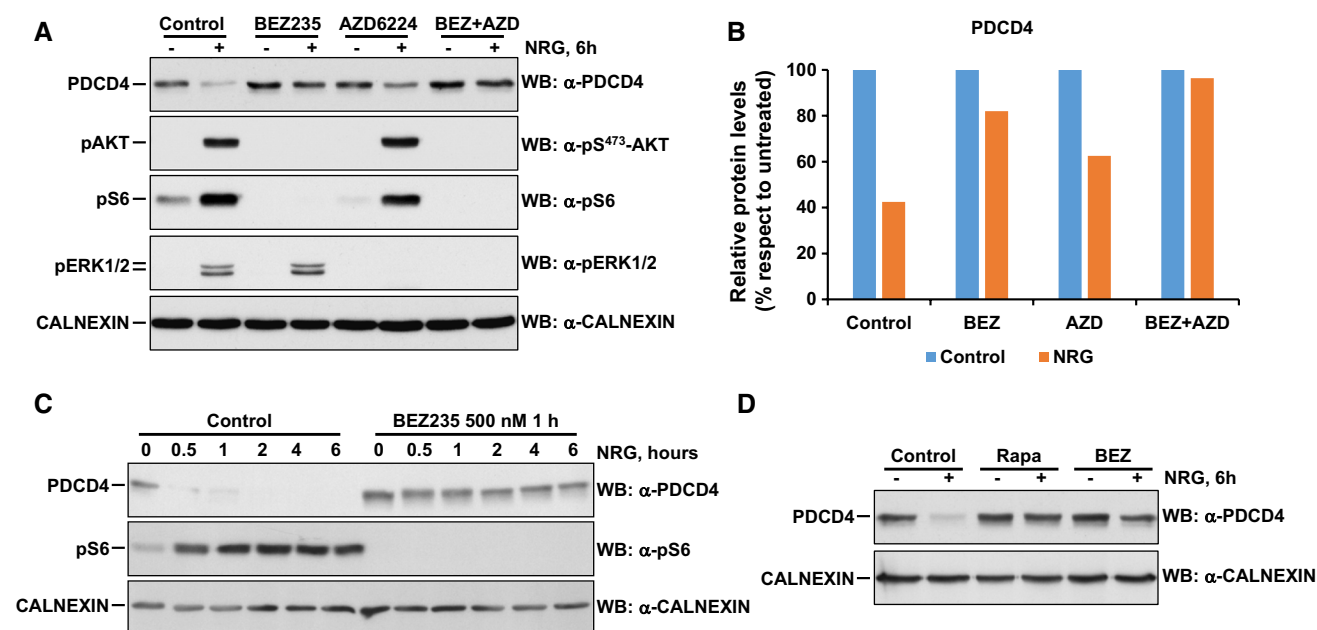
Fig. 6 NRG controls PDCD4 stability through several signaling routes. **a** MCF7 cells were preincubated with BEZ235 (1 μM), AZD6224 (5 μM) or a combination of BEZ235 plus AZD6224 for 3 h, and then treated without or with NRG (10 nM) during 6 h. Levels of PDCD4, pAKTS473, pS6, pERK1/2 and calnexin were analyzed by Western blotting. **b** Quantitative representation of the relative protein levels of PDCD4 respect to cells not treated with NRG in each condition of the experiment shown in **a**. **c** MCF7 cells were preincubated with BEZ235 (500 nM) and then treated without or with NRG for the times indicated. **d** Role of the mTORC1 pathway in the control of PDCD4 stability. MCF7 cells were preincubated with BEZ235 (1 μM) or rapamycin (100 nM) and then treated with or without NRG for 6 h

presence of NRG (Fig. 7b, c; supplementary Fig. 7a). On the other side, we transfected PDCD4 into MCF7 cells to increase its level over the endogenous one (Fig. 7d) and analyzed the effect of such increase on resting or NRG-induced migration. MCF7 cells overexpressing PDCD4 migrated less than the parental MCF7 cell line and its response to NRG was profoundly compromised (Fig. 7e; supplementary Fig. 7b).

The potential effect of PDCD4 on NRG-induced invasion was also explored. Knock down of PDCD4 favored the invading characteristics of MCF7 cells, both in the absence or presence of NRG (Fig. 7f). Interestingly, PDCD4 knock down augmented NRG-induced up-regulation of the metalloprotease collagenase-3 (also known as MMP13) (Fig. 7g), which has been reported to play an important role in NRG-induced local as well as distant dissemination [34].

One of the relevant actions of NRG on breast cancer cells is the stimulation of cell proliferation. To investigate the role of PDCD4 in the proliferative responses upon activation of NRG receptors, the effect of overexpressing HA-tagged PDCD4 was explored in MCF7 and T47D cells (Fig. 7h; supplementary Fig. 7c, d). Increased expression of PDCD4 decreased the resting and NRG-induced proliferation of MCF7 and T47D cells.

Discussion

Identification of intermediates that participate in NRG-ErbB signaling is critical for understanding how this ligand-receptor system regulates basic physiological functions such as heart and peripheral nervous system homeostasis. In addition, given the relevance of such system in certain diseases such as cancer or schizophrenia, advances in such understanding are required to assess whether pharmacological action on these intermediates may offer therapeutic benefits. In searching for intermediates of this signaling pathway, using genomic as well as proteomic approaches, we formerly involved ERK5, P-REX1 and MMP13 in different prooncogenic actions of the NRG-ErbB signaling axis [31, 33, 34]. Here we describe the identification of a novel and relevant intermediate of that signaling pathway, the PDCD4 protein.

PDCD4 was initially described in mouse cells treated with dexamethasone and was associated to programmed cell death [50]. Several studies have confirmed the role of this protein in cell death but have also unveiled a multifaceted role of that protein in the regulation of several prooncogenic characteristics (reviewed in [46, 51]). Thus, PDCD4 has been shown to inhibit proliferation, invasion or metastasis, gaining acceptance as a tumor suppressor protein [52].
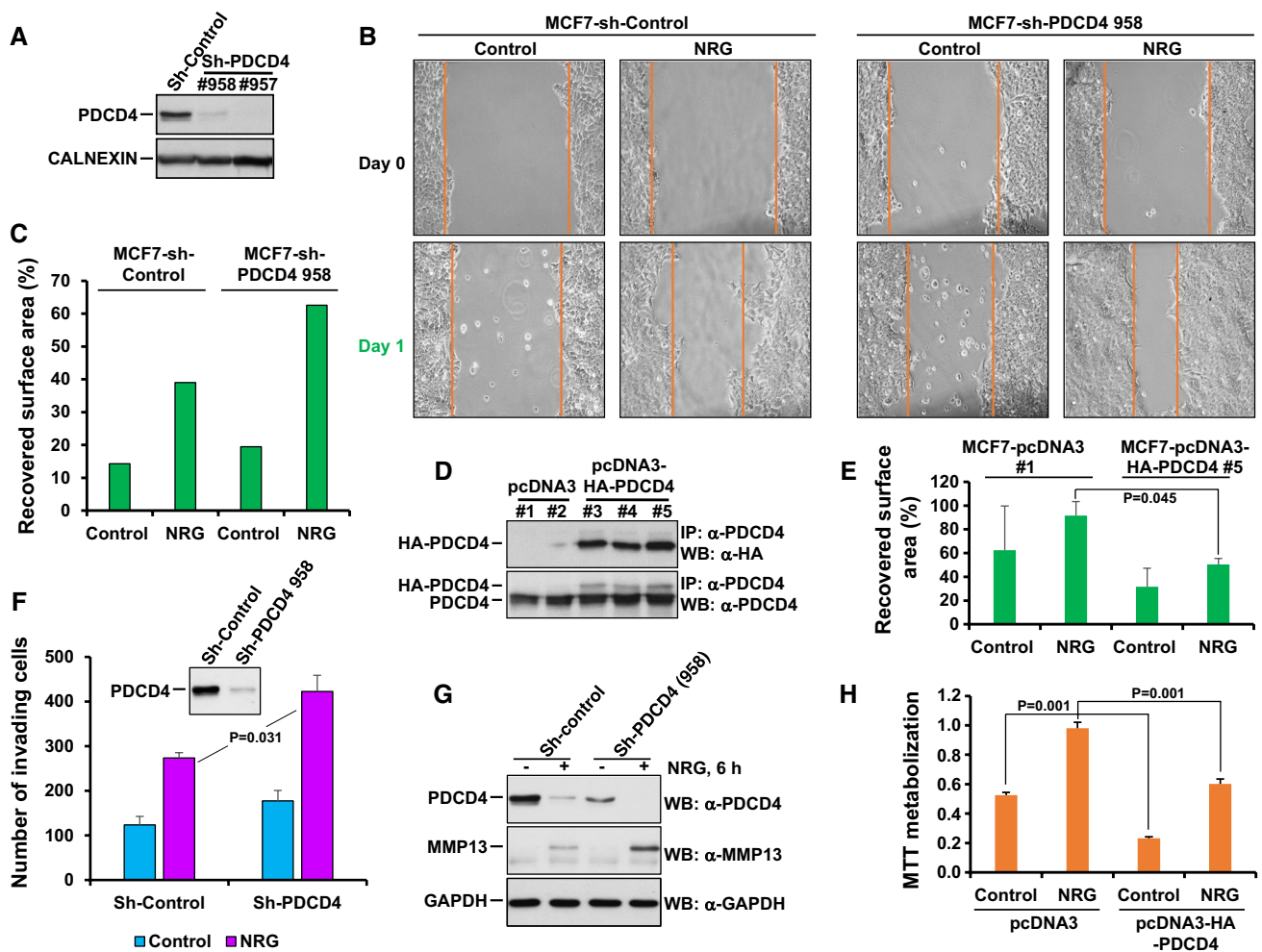
Fig. 7 Control of NRG-induced migration, invasion and proliferation by PDCD4. **a** Knockdown of PDCD4 in MCF7 cells. Cells were infected with lentivirus containing the shRNA control (Sh-Control) or two shRNA sequences targeting PDCD4. Levels of PDCD4 were analyzed by Western blotting, using calnexin as a loading control. **b** Representative images from the wound healing assay showing the effect of PDCD4 knockdown on NRG-induced migration of MCF7 cells. The colored lines delimit the wounded region area. **c** Bar graph representing the recovered surface area with respect to the initial wounded area in each condition of the experiment performed in **b**. **d** Overexpression of PDCD4 in MCF7 cells. Clones of MCF7 cells transfected with HA-PDCD4 or empty vector were lysed and expression of the exogenous HA-PDCD4 or endogenous PDCD4 detected by Western.

e Increased expression of PDCD4 prevented NRG-induced migration. The bar graph represents the recovered surface area with respect to the initial area in each condition. **f** Bar graph showing the number of MCF7-sh-Control or MCF7-sh-PDCD4 invading cells 48 h after NRG stimulation. Invading cells (those able to pass through the Matrigel layer) were fixed, stained with crystal violet, and counted. The Western image above the graph shows the level of PDCD4 in MCF7-sh-Control or MCF7-sh-PDCD4 cells. **g** Western blotting analysis of the effect of PDCD4 knockdown on the regulation of MMP13 after NRG stimulation for 6 h in MCF7 cells. **h** Increased expression of PDCD4 decreased resting and NRG-induced proliferation of MCF7 cells. Cell proliferation was determined by MTT metabolization 3 days after NRG (10 nM) stimulation

The process of identification of PDCD4 as an NRG-ErbB signaling intermediate started with the observation that an antibody generated against a phosphorylated version of P-REX1 cross-reacted with a phosphoprotein of 60 kDa. Proteomic analyses identified p60 as PDCD4. Further molecular analyses defined serine 67 as the site recognized by the anti-phospho-P-REX1 antibody. Inspection of the peptide sequence against which the p-P-REX1 antibody was raised and the sequence surrounding serine 67 showed little primary homology between both peptides. Therefore,

additional conformational determinants beyond the primary sequence may contribute to favor the cross reactivity of the anti-P-REX1 antibody with pPDCD4. In our model system, the signal responsible for S^{67} phosphorylation upon activation of NRG receptors was conveyed through the PI3K/mTOR and the classical ERK1/2 MAPK route, as indicated by pharmacological manipulation of both routes. Neutralization of signaling of each individual route, using the upstream inhibitors of these routes BEZ235 or AZD6244, had a poor effect on NRG-induced S^{67} phosphorylation of

PDCD4. However, combined treatment with those agents efficiently inhibited NRG-induced S^{67} phosphorylation of PDCD4. These results indicate that signals from NRG receptors responsible for such phosphorylation can be transduced through both routes and the inhibition of one of them allows the other to still transduce the phosphorylation signal, compensating the loss of signaling by the inhibited pathway. Such compensatory PDCD4 regulation by NRG-ErbB receptors may reflect a need for strict regulation of PDCD4 function during signaling once ErbB receptors are activated. Further pharmacological studies suggested that S6K and p90RSK may be involved in the regulation of S^{67} phosphorylation of PDCD4 by NRG receptors. Evidence for the involvement of S6K (downstream of PI3K/mTOR) in S^{67} phosphorylation of PDCD4 has already been provided, as well as a role for AKT in such phosphorylation [40, 44]. In addition, p90RSK has been reported to participate in the phosphorylation of PDCD4 in serines 76 and 457 [39, 41], but not in S^{67} phosphorylation. We, however, demonstrate here that p90RSK participates in NRG-induced S^{67} phosphorylation. In contrast, AKT was excluded as a potential mediator in the action of NRG since inhibitors of AKT did not prevent NRG-induced S^{67} phosphorylation of PDCD4. While our studies cannot define whether S6K and p90RSK kinases act directly on PDCD4, the inhibitor studies confirm their participation in the control of S^{67} phosphorylation of PDCD4. Moreover, our data define for the first time to p90RSK as a kinase controlling S^{67} phosphorylation of PDCD4. Interestingly, S^{67} lies within the consensus sequence RXRXXS/T recognized by both S6K1 and RSK [46].

Serine 67 of PDCD4 is located in a region of the protein implicated in its stability [51, 52]. In fact, previous reports have demonstrated that phosphorylation of nearby serine 76 regulates PDCD4 stability [39, 41]. Therefore, the possibility that NRG could affect PDCD4 stability through S^{67} phosphorylation appeared likely. In fact, activation of NRG receptors caused PDCD4 downregulation. This action was evident after a few hours of treatment with NRG and was sustained over time. Such degradation of PDCD4 was caused by the proteasome, as indicated by results using the proteasome inhibitor MG132, and required nucleocytoplasmic movement of PDCD4. In fact, leptomycin B, which blocks exit of proteins from the nucleus [43], inhibited degradation of PDCD4. Such effect of NRG on PDCD4 levels appeared to be mediated by phosphorylation-induced degradation of the protein, since a version of PDCD4 in which serine 67 was mutated to alanine, resisted NRG-induced degradation. In addition, pharmacologic studies indicated that agents acting on the pathways that control S^{67} phosphorylation of PDCD4 could prevent NRG-induced degradation of PDCD4. Especially effective in this inhibitory action were agents that target the PI3K/mTORC1 route, indicating a predominant

role of such route in the control of PDCD4 stability. These findings are especially relevant from the translational point of view. Thus, the inhibitory effect of rapamycin on the degradation of PDCD4 may help in understanding the antitumoral properties of mTORC1 inhibitors used in the oncology clinic. These results are in line with reported data indicating that PDCD4 phosphorylation at S^{67} facilitates its recognition by the E3 ligase β-transducin repeats containing protein, leading to proteasomal degradation [40]. Another report suggested that S^{457} phosphorylation of PDCD4 was required for nuclear translocation of PDCD4 [44]. While we could confirm that mutation of S^{457} prevented nuclear localization and translocation of PDCD4 (data not shown), mutation of S^{67} did not prevent nuclear localization of PDCD4, in agreement with a former report [44]. Together, these data indicate that NRG-induced phosphorylation of PDCD4 at S^{67} promotes proteasomal degradation of PDCD4, which requires its export outside the nucleus. It cannot be excluded that in addition to proteasomal degradation, NRG may also affect PDCD4 levels by downregulation of its mRNA in analogy to such effect caused by EGF in other cell types [53]. The effect of NRG on PDCD4 phosphorylation and degradation was observed in several breast cancer cell lines bearing different levels of ErbB receptors. It is however important to mention that in SKBR3 cells, agents that neutralize the kinase activity of HER2 provoked an increase in PDCD4, suggesting that constitutive signaling by overexpressed HER2 maintains low levels of PDCD4 in this cell line. Therefore, either ligand-stimulated or overexpressed and constitutively active ErbB receptors may signal through the PI3K and ERK routes to diminish the inhibitory function of PDCD4 on the oncogenic properties of breast cancer cells.

Functional studies performed to define the role of PDCD4 in NRG-induced biological responses demonstrated that PDCD4 exerts a critical role in the transduction of signals that affect the prooncogenic actions of the ErbB system. Genetic manipulation of PDCD4 levels showed that MCF7 cells in which levels of PDCD4 were down regulated by shRNA migrated more and invaded more than MCF7 cells expressing autochthonous levels. Such result indicated that PDCD4 restrained migration and invasion in these cells and sustained a role of PDCD4 as a tumor suppressor, a characteristic that was also supported by the restriction of resting and NRG-induced proliferation of MCF7 and T47D cells overexpressing PDCD4.

The work herewith reported situates PDCD4 within the complex map of NRG-ErbB signaling. Due to the roles of this ligand-receptor system in biology and in pathophysiology, our findings should help in understanding the signaling upon activation of NRG receptors, and may indeed facilitate the optimization of certain therapies, for example by stabilizing PDCD4 levels using clinically available PI3K/

mTOR inhibitors in combination with agents that directly target the ErbB receptors. Importantly, inhibitors of HER2 augmented PDCD4 levels in breast cancer cells overexpressing HER2 offering preclinical rationale for the combination of agents that target HER2 and mTORC1 for the treatment of patients with that type of breast tumors. In any case, the finding that PDCD4 plays an important role in important oncogenic properties such as migration, invasion or proliferation, which are controlled by NRG receptors opens the possibility of therapeutically manipulating PCD4 levels in tumors fed by the NRG-ErbB system.

Compliance with ethical standards

Conflict of interest The authors declare that they have no conflict of interest.

References

1. Arteaga CL, Engelman JA (2014) ERBB receptors: from oncogene discovery to basic science to mechanism-based cancer therapeutics. Cancer Cell 25(3):282–303. https://doi.org/10.1016/j.ccr.2014.02.025

2. Massague J, Pandiella A (1993) Membrane-anchored growth factors. Annu Rev Biochem 62:515–541. https://doi.org/10.1146/annurev.bi.62.070193.002503

3. Montero JC, Rodriguez-Barrueco R, Ocana A, Diaz-Rodriguez E, Esparis-Ogando A, Pandiella A (2008) Neuregulins and cancer. Clin Cancer Res 14(11):3237–3241. https://doi.org/10.1158/1078-0432.CCR-07-5133

4. Meyer D, Birchmeier C (1995) Multiple essential functions of neuregulin in development. Nature 378(6555):386–390. https://doi.org/10.1038/378386a0

5. Britsch S, Li L, Kirchhoff S, Theuring F, Brinkmann V, Birchmeier C, Riethmacher D (1998) The ErbB2 and ErbB3 receptors and their ligand, neuregulin-1, are essential for development of the sympathetic nervous system. Genes Dev 12(12):1825–1836. https://doi.org/10.1101/gad.12.12.1825

6. Meyer D, Yamaai T, Garratt A, Riethmacher-Sonnenberg E, Kane D, Theill LE, Birchmeier C (1997) Isoform-specific expression and function of neuregulin. Development 124(18):3575–3586

7. Montero JC, Yuste L, Diaz-Rodriguez E, Esparis-Ogando A, Pandiella A (2000) Differential shedding of transmembrane neuregulin isoforms by the tumor necrosis factor-alpha-converting enzyme. Mol Cell Neurosci 16(5):631–648. https://doi.org/10.1006/mcne.2000.0896

8. Montero JC, Rodriguez-Barrueco R, Yuste L, Juanes PP, Borges J, Esparis-Ogando A, Pandiella A (2007) The extracellular linker of pro-neuregulin-alpha2c is required for efficient sorting and juxtacrine function. Mol Biol Cell 18(2):380–393. https://doi.org/10.1091/mbc.e06-06-0511

9. Esparis-Ogando A, Montero JC, Arribas J, Ocana A, Pandiella A (2016) Targeting the EGF/HER ligand-receptor system in cancer. Curr Pharm Des 22(39):5887–5898. https://doi.org/10.2174/1381612822666160715132233

10. Hynes NE, MacDonald G (2009) ErbB receptors and signaling pathways in cancer. Curr Opin Cell Biol 21(2):177–184. https://doi.org/10.1016/j.ceb.2008.12.010

11. Birchmeier C (2009) ErbB receptors and the development of the nervous system. Exp Cell Res 315(4):611–618. https://doi.org/10.1016/j.yexcr.2008.10.035

12. Sibilia M, Steinbach JP, Stingl L, Aguzzi A, Wagner EF (1998) A strain-independent postnatal neurodegeneration in mice lacking the EGF receptor. EMBO J 17(3):719–731. https://doi.org/10.1093/emboj/17.3.719

13. Sibilia M, Wagner EF (1995) Strain-dependent epithelial defects in mice lacking the EGF receptor. Science 269(5221):234–238. https://doi.org/10.1126/science.7618085

14. Erickson SL, O'Shea KS, Ghaboosi N, Loverro L, Frantz G, Bauer M, Lu LH, Moore MW (1997) ErbB3 is required for normal cerebellar and cardiac development: a comparison with ErbB2-and heregulin-deficient mice. Development 124(24):4999–5011

15. Gassmann M, Casagranda F, Orioli D, Simon H, Lai C, Klein R, Lemke G (1995) Aberrant neural and cardiac development in mice lacking the ErbB4 neuregulin receptor. Nature 378(6555):390–394. https://doi.org/10.1038/378390a0

16. Lee KF, Simon H, Chen H, Bates B, Hung MC, Hauser C (1995) Requirement for neuregulin receptor erbB2 in neural and cardiac development. Nature 378(6555):394–398. https://doi.org/10.1038/378394a0

17. Riethmacher D, Sonnenberg-Riethmacher E, Brinkmann V, Yamaai T, Lewin GR, Birchmeier C (1997) Severe neuropathies in mice with targeted mutations in the ErbB3 receptor. Nature 389(6652):725–730. https://doi.org/10.1038/39593

18. Krane IM, Leder P (1996) NDF/heregulin induces persistence of terminal end buds and adenocarcinomas in the mammary glands of transgenic mice. Oncogene 12(8):1781–1788

19. Fernandez-Cuesta L, Plenker D, Osada H, Sun R, Menon R, Leenders F, Ortiz-Cuaran S, Peifer M, Bos M, Dassler J, Malchers F, Schottle J, Vogel W, Dahmen I, Koker M, Ullrich RT, Wright GM, Russell PA, Wainer Z, Solomon B, Brambilla E, Nagy-Mignotte H, Moro-Sibilot D, Brambilla CG, Lantuejoul S, Altmuller J, Becker C, Nurnberg P, Heuckmann JM, Stoelben E, Petersen I, Clement JH, Sanger J, Muscarella LA, la Torre A, Fazio VM, Lahortiga I, Perera T, Ogata S, Parade M, Brehmer D, Vingron M, Heukamp LC, Buettner R, Zander T, Wolf J, Perner S, Ansen S, Haas SA, Yatabe Y, Thomas RK (2014) CD74-NRG1 fusions in lung adenocarcinoma. Cancer Discov 4(4):415–422. https://doi.org/10.1158/2159-8290.CD-13-0633

20. Murayama T, Nakaoku T, Enari M, Nishimura T, Tominaga K, Nakata A, Tojo A, Sugano S, Kohno T, Gotoh N (2016) Oncogenic fusion gene CD74-NRG1 confers cancer stem cell-like properties in lung cancer through a IGF2 autocrine/paracrine circuit. Cancer Res 76(4):974–983. https://doi.org/10.1158/0008-5472.CAN-15-2135

21. Pan Y, Zhang Y, Ye T, Zhao Y, Gao Z, Yuan H, Zheng D, Zheng S, Li H, Li Y, Jin Y, Sun Y, Chen H (2019) Detection of novel

NRG1, EGFR, and MET fusions in lung adenocarcinomas in the Chinese population. J Thorac Oncol 14(11):2003–2008. https://doi.org/10.1016/j.jtho.2019.07.022

22. Heining C, Horak P, Uhrig S, Codo PL, Klink B, Hutter B, Frohlich M, Bonekamp D, Richter D, Steiger K, Penzel R, Endris V, Ehrenberg KR, Frank S, Kleinheinz K, Toprak UH, Schlesner M, Mandal R, Schulz L, Lambertz H, Fetscher S, Bitzer M, Malek NP, Horger M, Giese NA, Strobel O, Hackert T, Springfeld C, Feuerbach L, Bergmann F, Schrock E, von Kalle C, Weichert W, Scholl C, Ball CR, Stenzinger A, Brors B, Frohling S, Glimm H (2018) NRG1 fusions in KRAS wild-type pancreatic cancer. Cancer Discov 8(9):1087–1095. https://doi.org/10.1158/2159-8290.CD-18-0036

23. Cheema PK, Doherty M, Tsao MS (2017) A case of invasive mucinous pulmonary adenocarcinoma with a CD74-NRG1 fusion protein targeted with afatinib. J Thorac Oncol 12(12):e200–e202. https://doi.org/10.1016/j.jtho.2017.07.033

24. Drilon A, Somwar R, Mangatt BP, Edgren H, Desmeules P, Ruusulehto A, Smith RS, Delasos L, Vojnic M, Plodkowski AJ, Sabari J, Ng K, Montecalvo J, Chang J, Tai H, Lockwood WW, Martinez V, Riely GJ, Rudin CM, Kris MG, Arcila ME, Matheny C, Benayed R, Rekhtman N, Ladanyi M, Ganji G (2018) Response to ERBB3-directed targeted therapy in NRG1-rearranged cancers. Cancer Discov 8(6):686–695. https://doi.org/10.1158/2159-8290.CD-17-1004

25. Jones MR, Lim H, Shen Y, Pleasance E, Ch'ng C, Reisle C, Leelakumari S, Zhao C, Yip S, Ho J, Zhong E, Ng T, Ionescu D, Schaeffer DF, Mungall AJ, Mungall KL, Zhao Y, Moore RA, Ma Y, Chia S, Ho C, Renouf DJ, Gelmon K, Jones SJM, Marra MA, Laskin J (2017) Successful targeting of the NRG1 pathway indicates novel treatment strategy for metastatic cancer. Ann Oncol 28(12):3092–3097. https://doi.org/10.1093/annonc/mdx523

26. de Alava E, Ocana A, Abad M, Montero JC, Esparis-Ogando A, Rodriguez CA, Otero AP, Hernandez T, Cruz JJ, Pandiella A (2007) Neuregulin expression modulates clinical response to trastuzumab in patients with metastatic breast cancer. J Clin Oncol 25(19):2656–2663. https://doi.org/10.1200/JCO.2006.08.6850

27. Ocana A, Diez-Gonzalez L, Esparis-Ogando A, Montero JC, Amir E, Pandiella A (2016) Neuregulin expression in solid tumors: prognostic value and predictive role to anti-HER3 therapies. Oncotarget 7(29):45042–45051. https://doi.org/10.18632/oncotarget.8648

28. Slamon DJ, Clark GM, Wong SG, Levin WJ, Ullrich A, McGuire WL (1987) Human breast cancer: correlation of relapse and survival with amplification of the HER-2/neu oncogene. Science 235(4785):177–182. https://doi.org/10.1126/science.3798106

29. Bailey MH, Tokheim C, Porta-Pardo E, Sengupta S, Bertrand D, Weerasinghe A, Colaprico A, Wendl MC, Kim J, Reardon B, Kwok-Shing Ng P, Jeong KJ, Cao S, Wang Z, Gao J, Gao Q, Wang F, Liu EM, Mularoni L, Rubio-Perez C, Nagarajan N, Cortes-Ciriano I, Zhou DC, Liang WW, Hess JM, Yellapantula VD, Tamborero D, Gonzalez-Perez A, Suphavilai C, Ko JY, Khurana E, Park PJ, Van Allen EM, Liang H, Group MCW, Cancer Genome Atlas Research N, Lawrence MS, Godzik A, Lopez-Bigas N, Stuart J, Wheeler D, Getz G, Chen K, Lazar AJ, Mills GB, Karchin R, Ding L (2018) Comprehensive characterization of cancer driver genes and mutations. Cell 174(4):1034–1035. https://doi.org/10.1016/j.cell.2018.07.034

30. Hyman DM, Piha-Paul SA, Won H, Rodon J, Saura C, Shapiro GI, Juric D, Quinn DI, Moreno V, Doger B, Mayer IA, Boni V, Calvo E, Loi S, Lockhart AC, Erinjeri JP, Scaltriti M, Ulaner GA, Patel J, Tang J, Beer H, Selcuklu SD, Hanrahan AJ, Bouvier N, Melcer M, Murali R, Schram AM, Smyth LM, Jhaveri K, Li BT, Drilon A, Harding JJ, Iyer G, Taylor BS, Berger MF, Cutler RE Jr, Xu F, Butturini A, Eli LD, Mann G, Farrell C, Lalani AS, Bryce RP, Arteaga CL, Meric-Bernstam F, Baselga

J, Solit DB (2018) HER kinase inhibition in patients with HER2- and HER3-mutant cancers. Nature 554(7691):189–194. https://doi.org/10.1038/nature25475

31. Esparis-Ogando A, Diaz-Rodriguez E, Montero JC, Yuste L, Crespo P, Pandiella A (2002) Erk5 participates in neuregulin signal transduction and is constitutively active in breast cancer cells overexpressing ErbB2. Mol Cell Biol 22(1):270–285. https://doi.org/10.1128/mcb.22.1.270-285.2002

32. Pandiella A, Montero JC (2013) Molecular pathways: P-Rex in cancer. Clin Cancer Res 19(17):4564–4569. https://doi.org/10.1158/1078-0432.CCR-12-1662

33. Montero JC, Seoane S, Ocana A, Pandiella A (2011) P-Rex1 participates in neuregulin-ErbB signal transduction and its expression correlates with patient outcome in breast cancer. Oncogene 30(9):1059–1071. https://doi.org/10.1038/onc.2010.489

34. Seoane S, Montero JC, Ocana A, Pandiella A (2016) Breast cancer dissemination promoted by a neuregulin-collagenase 3 signalling node. Oncogene 35(21):2756–2765. https://doi.org/10.1038/onc.2015.337

35. Orive-Ramos A, Seoane S, Ocana A, Pandiella A, Montero JC (2017) Regulation of the prometastatic neuregulin-MMP13 axis by SRC family kinases: therapeutic implications. Mol Oncol 11(12):1788–1805. https://doi.org/10.1002/1878-0261.12145

36. Esparis-Ogando A, Alegre A, Aguado B, Mateo G, Gutierrez N, Blade J, Schenkein D, Pandiella A, San Miguel JF (2005) Bortezomib is an efficient agent in plasma cell leukemias. Int J Cancer 114(4):665–667. https://doi.org/10.1002/ijc.20793

37. Montero JC, Yuste L, Diaz-Rodriguez E, Esparis-Ogando A, Pandiella A (2002) Mitogen-activated protein kinase-dependent and -independent routes control shedding of transmembrane growth factors through multiple secretases. Biochem J 363(Pt 2):211–221. https://doi.org/10.1042/0264-6021:3630211

38. Montero JC, Seoane S, Pandiella A (2013) Phosphorylation of P-Rex1 at serine 1169 participates in IGF-1R signaling in breast cancer cells. Cell Signal 25(11):2281–2289. https://doi.org/10.1016/j.cellsig.2013.07.018

39. Cuesta R, Holz MK (2016) RSK-mediated down-regulation of PDCD4 is required for proliferation, survival, and migration in a model of triple-negative breast cancer. Oncotarget 7(19):27567–27583. https://doi.org/10.18632/oncotarget.8375

40. Dorrello NV, Peschiaroli A, Guardavaccaro D, Colburn NH, Sherman NE, Pagano M (2006) S6K1- and betaTRCP-mediated degradation of PDCD4 promotes protein translation and cell growth. Science 314(5798):467–471. https://doi.org/10.1126/science.1130276

41. Galan JA, Geraghty KM, Lavoie G, Kanshin E, Tcherkezian J, Calabrese V, Jeschke GR, Turk BE, Ballif BA, Blenis J, Thibault P, Roux PP (2014) Phosphoproteomic analysis identifies the tumor suppressor PDCD4 as a RSK substrate negatively regulated by 14-3-3. Proc Natl Acad Sci USA 111(29):E2918–2927. https://doi.org/10.1073/pnas.1405601111

42. Bohm M, Sawicka K, Siebrasse JP, Brehmer-Fastnacht A, Peters R, Klempnauer KH (2003) The transformation suppressor protein Pdcd4 shuttles between nucleus and cytoplasm and binds RNA. Oncogene 22(31):4905–4910. https://doi.org/10.1038/sj.onc.1206710

43. Kudo N, Matsumori N, Taoka H, Fujiwara D, Schreiner EP, Wolff B, Yoshida M, Horinouchi S (1999) Leptomycin B inactivates CRM1/exportin 1 by covalent modification at a cysteine residue in the central conserved region. Proc Natl Acad Sci USA 96(16):9112–9117. https://doi.org/10.1073/pnas.96.16.9112

44. Palamarchuk A, Efanov A, Maximov V, Aqeilan RI, Croce CM, Pekarsky Y (2005) Akt phosphorylates and regulates Pdcd4 tumor suppressor protein. Cancer Res 65(24):11282–11286. https://doi.org/10.1158/0008-5472.CAN-05-3469

45. Sapkota GP, Cummings L, Newell FS, Armstrong C, Bain J, Frodin M, Grauert M, Hoffmann M, Schnapp G, Steegmaier M, Cohen P, Alessi DR (2007) BI-D1870 is a specific inhibitor of the p90 RSK (ribosomal S6 kinase) isoforms in vitro and in vivo. Biochem J 401(1):29–38. https://doi.org/10.1042/bj20061088

46. Matsuhashi S, Manirujjaman M, Hamajima H, Ozaki I (2019) Control mechanisms of the tumor suppressor PDCD4: expression and functions. Int J Mol Sci. https://doi.org/10.3390/ijms20092304

47. Hirai H, Sootome H, Nakatsuru Y, Miyama K, Taguchi S, Tsujioka K, Ueno Y, Hatch H, Majumder PK, Pan BS, Kotani H (2010) MK-2206, an allosteric Akt inhibitor, enhances antitumor efficacy by standard chemotherapeutic agents or molecular targeted drugs in vitro and in vivo. Mol Cancer Ther 9(7):1956–1967. https://doi.org/10.1158/1535-7163.mct-09-1012

48. Yip CK, Murata K, Walz T, Sabatini DM, Kang SA (2010) Structure of the human mTOR complex I and its implications for rapamycin inhibition. Mol Cell 38(5):768–774. https://doi.org/10.1016/j.molcel.2010.05.017

49. Wang Q, Zhu J, Zhang Y, Sun Z, Guo X, Wang X, Lee E, Bakthavatchalu V, Yang Q, Yang HS (2013) Down-regulation of programmed cell death 4 leads to epithelial to mesenchymal transition and promotes metastasis in mice. Eur J Cancer 49(7):1761–1770. https://doi.org/10.1016/j.ejca.2012.12.014

50. Shibahara K, Asano M, Ishida Y, Aoki T, Koike T, Honjo T (1995) Isolation of a novel mouse gene MA-3 that is induced upon programmed cell death. Gene 166(2):297–301. https://doi.org/10.1016/0378-1119(95)00607-9

51. Wang Q, Yang HS (2018) The role of Pdcd4 in tumour suppression and protein translation. Biol Cell. https://doi.org/10.1111/boc.201800014

52. Lankat-Buttgereit B, Goke R (2009) The tumour suppressor Pdcd4: recent advances in the elucidation of function and regulation. Biol Cell 101(6):309–317. https://doi.org/10.1042/BC20080191

53. Matsuhashi S, Hamajima H, Xia J, Zhang H, Mizuta T, Anzai K, Ozaki I (2014) Control of a tumor suppressor PDCD4: Degradation mechanisms of the protein in hepatocellular carcinoma cells. Cell Signal 26(3):603–610. https://doi.org/10.1016/j.cellsig.2013.11.038